Structures 64 (2024) 106490

Contents lists available at ScienceDirect

Structures

journal homepage: www.elsevier.com/locate/structures

An analytical matrix approach for the prediction of the elastic lateral displacements of CLT platform-type lateral load resisting systems

Daniele Casagrande [a], Giuseppe D'Arenzo [c,*], Mohammad Masroor [b], Igor Gavrić [d], Ghasan Doudak [b]

[a] Department of Civil, Environmental and Mechanical Engineering, University of Trento, via Mesiano, 77, 38123 Trento, Italy
[b] Faculty of Civil Engineering, University of Ottawa, 161 Louis-Pasteur Pièce, Ottawa, ON K1N 6N5, Canada
[c] Department of Civil and Architectural Engineering, Aarhus University, Inge Lehmanns Gade, 10, 8000 Aarhus C, Denmark
[d] InnoRenew CoE, Livade 6a, 6310 Izola, Slovenia & Faculty of Mathematics, Natural Sciences and Information Technologies, University of Primorska, Glagoljaška ulica 8, 6000 Koper, Slovenia

ARTICLE INFO

Keywords:
Cross Laminated Timber
Shear-wall
Lateral displacement
Lateral load
Stiffness
Mass Timber

ABSTRACT

This study presents an analytical method for the elastic lateral displacement calculation of platform-type cross laminated timber (CLT) lateral load resisting systems using a matrix approach. The current state-of-the-art models for lateral deflection calculation of single- and multi-panel CLT shear-walls systems were extended from single-storey cases to generalized multi-storey multi-panel CLT shear-wall systems. The proposed calculation method was validated against tests on twelve single-storey shear-walls and one two-storey shear-wall from four previously conducted experimental campaigns. The 2D lateral displacement analytical calculation model was then further expanded to the 3D application for CLT lateral load resisting systems through a matrix approach. The matrix method was verified against an analytical-numerical comparison on two case studies. The proposed analytical model forms a solid foundation for a potential implementation of this lateral deflection model for CLT shear-wall systems in the next generation of standards such as Eurocode 5 and CSA O86.

1. Introduction and objectives

Cross laminated timber (CLT) is a versatile engineered wood product (EWP) that has been present in the construction landscape for the past three decades. Significant developments have been made in terms of production and technology, developing basic characteristic material properties, proposing design methods [3], as well as establishing performance in seismic-prone areas [25]. The use of CLT as a structural material has been prevalent in low-rise buildings, while increasingly penetrating the mid-rise and tall building market [33,39].

Due to the relative lightweight and flexible nature of CLT structures, lateral deflection may become the governing criteria in design of structural members, as well as connections in multi-storey CLT buildings. Although design methods for the ultimate limit state design of CLT shear-wall systems have been reasonably well-established (e.g. [15]), research on establishing the lateral deflection has been lacking, and calculation procedures are not yet available in current versions of timber design standards (e.g., [6,10]).

CLT shear-walls in platform-type construction typically comprise of single- or multi-panels, where single-panel walls can be considered as monolithic, whereas multi-panel walls consist of two or more aligned wall panels, typically connected together with mechanical fasteners. The choice of multi-panel CLT shear-walls may be motivated by material efficiency in case of walls with window and door openings, and limitations associated with manufacturing and transportation size limits. More importantly, in seismic design, where capacity design principles need to be met, multi-panel CLT shear-walls provide superior behaviour in terms of energy dissipation and controlled failure sequence and mechanism, due to higher deformation capacity exhibited in those systems, compared to single-panel walls [14].

Several analytical models are currently available in the literature for the evaluation of the elastic lateral displacement of single-storey CLT shear-walls. Lukacs et al. [20] compared the state-of-the-art analytical approaches, and reported that the most significant deformation contributions of CLT single-panel shear-walls without openings are attributed to the flexibility of the connections (e.g. hold-downs and angle brackets), used to connect the CLT shear-walls to the foundation or to the storey below. It was also reported that the proposed methods differ

* Corresponding author.
E-mail addresses: daniele.casagrande@unitn.it (D. Casagrande), giuseppe.darenzo@cae.au.dk (G. D'Arenzo).

https://doi.org/10.1016/j.istruc.2024.106490
Received 5 December 2023; Received in revised form 12 April 2024; Accepted 25 April 2024
Available online 11 May 2024

from one-another mainly in the calculation of the lever arm used to calculate the compressive deformations at the wall panel edge in the rocking kinematic mode, as well as the assumptions related to assigning uni- or bi-directional behavioural characteristics to the mechanical anchors. For multi-panel shear-walls, most analytical proposals have been developed for two-panel CLT shear-walls (e.g., [12,13]) while a more general approach involving *m*-panels was developed by Casagrande et al. [5]. Complete proposals accounting for multi-storey effects such as lateral deflection contributions due to cumulative rotation and the flexibility of floor-to-wall connections have, so far, not been presented.

The effects of the structural interactions between shear-wall segments and other structural elements (i.e. floors and perpendicular walls) on the lateral response of CLT shear-walls have been investigated. The effect of the floor diaphragm on the rocking behavior of two-panel CLT shear-walls was investigated by Tamagnone et al. [37]. The results showed that the floor-to-wall connection played a significant role in the response of the analysed shear-wall whereas the out-of-plane bending stiffness of the CLT floor panel had a negligible effect. Similarly, Ruggeri et al. [32] conducted parametric numerical analyses to investigate the influence of the floor-to-wall connection on the mechanical behaviour of CLT shear-walls with openings. The interaction between CLT shear-walls and perpendicular walls was studied by Gavrić and Popovski [15] and Ruggeri et al. [31]. It was demonstrated that the contribution of the hold-down anchored to the perpendicular wall may significantly contribute to increase in the rocking stiffness and strength capacity of CLT shear-walls when adequate wall-to-wall connections are adopted to transfer the shear load between the two perpendicular CLT panels.

The main aim of this paper is to propose a general analytical approach to be implemented in the design of platform-type CLT shear-wall lateral load resisting systems, in order to facilitate the calculation of the elastic lateral displacement of multi-storey CLT shear-walls consisting of single- or multi-panel walls. In the proposed model, angle brackets' contribution can be considered as uni-directional (shear) or bi-directional (shear and tension), while hold-downs are considered to be uni-directional (tension only). The analytical model can also be applicable to CLT shear-wall systems with openings in cases where the wall consists of assemblies of wall segments, lintels and parapets, while walls with openings cut out of the panel are out of the scope of this study due to the higher degree of complexity in the stress distribution in the CLT panel. It should also be noted that the presented analytical model cannot be directly used for balloon-type shear-wall systems for which an adaptation of the analytical expressions would be necessary to consider the continuity of CLT panel along the height of the shear-wall. The effects of perpendicular walls and the interaction between shear-walls and floor diaphragms are also outside the scope of this study.

The specific objectives include: i) synthesizing the available analytical models for single- and multi-panel single storey CLT shear-walls; ii) extending the applicability of the models to multi-storey; iii) proposing a novel matrix approach for the elastic lateral displacement of multi-storey platform-type CLT lateral load resisting systems (LLRSs); and iv) providing an analytical approach which can be used by practitioners as an alternative to finite element models for the purpose of calculating the lateral displacements of CLT buildings, or by software developers to implement in structural analysis design software. The study contains novelties, discussed for the first time in the current paper, necessary to deal with lateral displacements of CLT multi-storey systems, such as the displacement contribution due to the floor-to-wall connections and to the cumulative rotation, discussed in Section 2, and the principle of the rocking displacement consistency, which is discussed in Section 3.3. The proposed analytical model is validated against twelve single-storey shear-walls and one two-storey shear-wall consisting of single- and multi-panel walls obtained from experimental test results. The expressions are also verified against a numerical model through two case-studies.

2. Lateral displacements of isolated multi-storey CLT shear-wall

2.1. General displacement behaviour

The total lateral displacement of an isolated multi-storey platform-type CLT shear-wall at the r^{th} storey, d_r, can be obtained as the cumulative inter-storey lateral displacements, δ_i, from the 1^{st} to the r^{th} storey, as presented in Eq. (1) and illustrated in Fig. 1 for a four-storey CLT building example.

$$d_r = \sum_{i=1}^{r} \delta_i \tag{1}$$

The inter-storey lateral displacement, δ_i, is obtained from the sum of six displacement contributions, as presented in Eq. 2, and shown in Fig. 2. These include: *i)* in-plane shear deformation of the CLT panel, $\delta_{S,i}$, *ii)* in-plane bending deformation of the CLT panel, $\delta_{B,i}$, *iii)* rigid body sliding of the shear-wall related to the lateral (shear) flexibility of the angle brackets, $\delta_{A,i}$, *iv)* sliding between the shear-wall under consideration and the floor above related to the flexibility of the floor-to-wall shear connections, $\delta_{F,i}$, *v)* rigid body rocking of the shear-wall related to the flexibility of vertical joints (for multi-panel shear-walls) and vertical (tensile) flexibility of the mechanical anchors (i.e. hold-down and angle brackets), $\delta_{R,i}$, and *vi)* the lateral displacement associated with the rotation of the storey below the wall under consideration (i.e., *(i-1)*th storey), $\delta_{\theta,i}$, which takes into account the cumulative rotation effects along the height of the multi-storey shear-wall.

$$\delta_i = \delta_{S,i} + \delta_{B,i} + \delta_{A,i} + \delta_{F,i} + \delta_{R,i} + \delta_{\theta,i} \tag{2}$$

The proposed analytical methodology to obtain the six contributions outlined in Eq. (2) is presented for single-panel and multi-panel CLT shear-walls with no openings, considering uni- or bi-directional behaviour of the angle-brackets.

The height and total length of the shear-wall under consideration at the i^{th} storey are defined as h_i and B_i, respectively, while the depth of the floor above the wall at the i^{th} storey is taken equal to $h_{floor,i}$. It is assumed that hold-downs are located at each end of the shear-wall, and n_a angle brackets are distributed along the total length of the shear-wall, (see Fig. 3).

The internal actions on the shear-wall at the i^{th} storey include the total lateral shear loads, V_i, total axial load due to gravity, N_i, total overturning moment acting at the bottom of the shear-wall due to the lateral loads, M_i, and the total overturning moment acting at the top of the shear-wall due to lateral loads, $M_{i,top}$, as illustrated in Fig. 3.

2.2. Displacement contributions for single-panel CLT shear-wall

2.2.1. Panel deformation

The inter-storey lateral displacement of a single-panel CLT shear-wall associated with the in-plane shear deformation of the panel, $\delta_{S,i}$, can be expressed as outlined in Eq. (3), according to Hummel et al. [16].

$$\delta_{S,i} = \frac{V_i \bullet h_i}{G_{eff,i} \bullet t_{CLT,i} \bullet B_i} \tag{3}$$

where $t_{CLT,i}$ is the total thickness of the CLT panel at the i^{th} storey and $G_{eff,i}$ is the effective in-plane shear modulus of the CLT panel, which can be calculated according to Brandner et al. [2], as expressed by Eq. (4).

$$G_{eff,i} = \frac{G_{0,i}}{1 + 6 \bullet \alpha_i \bullet \left(\frac{t_{mean,i}}{w_i}\right)^2} \tag{4}$$

where $G_{0,i}$ is the average in-plane shear modulus of the laminations, w_i is the width of the laminations or the distance between the edge and a groove in a lamination, and $t_{mean,i}$ is the mean thickness of laminations.

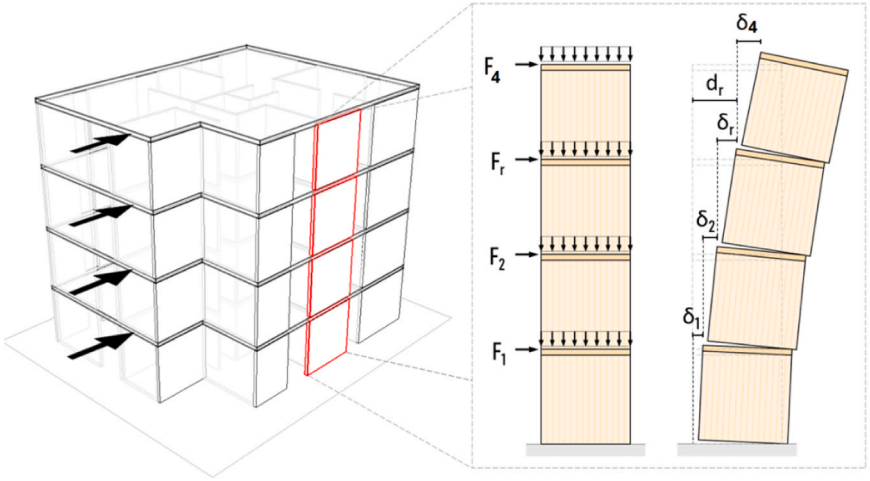

Fig. 1. Lateral displacements of a 4-storey isolated multi-storey platform-type CLT shear-wall.

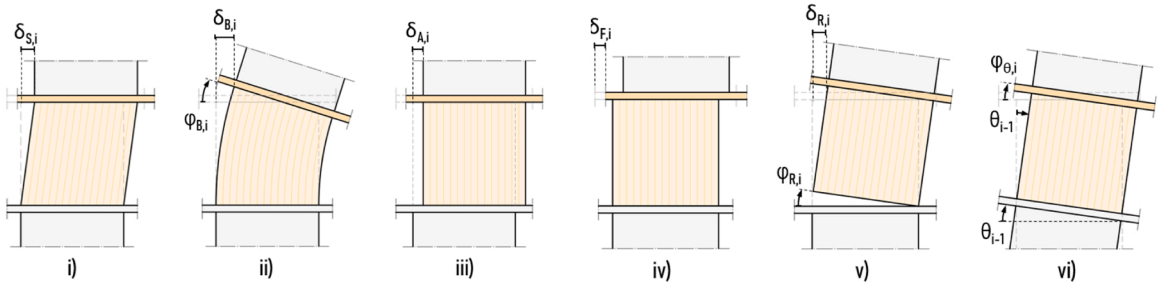

Fig. 2. In-plane displacement contributions. i) shear, ii) bending, iii) rigid body sliding, iv) sliding between shear-wall floor panel above, v) rigid body rocking, vi) rotation at top of the shear-wall at the storey below.

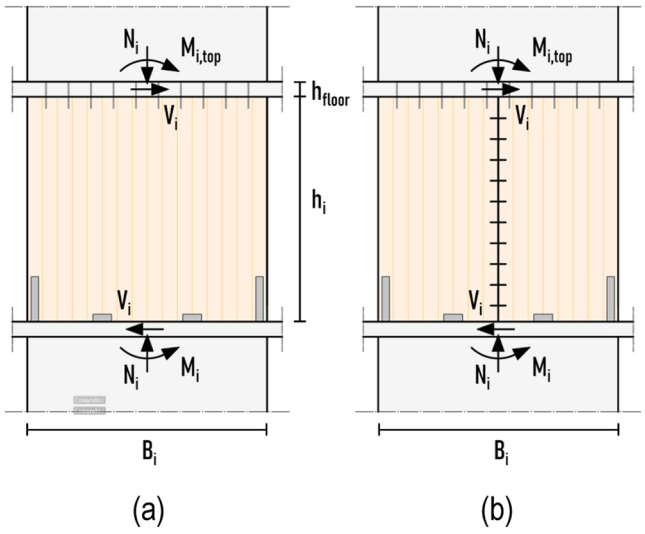

Fig. 3. Internal actions on single-panel (a) and multi-panel (b) shear-wall at the i-th storey.

The parameter α_i can be calculated using Eq. (5), where values of p are taken equal to 0.535 and 0.425 for a three- and five-ply CLT panel, respectively.

$$\alpha_i = p \bullet \left(\frac{t_{mean.i}}{w_i}\right)^{-0.79} \tag{5}$$

The inter-storey lateral displacement due to panel bending deformation, $\delta_{B,i}$, can be obtained from the beam theory, as expressed in Eq. (6).

$$\delta_{B,i} = \frac{M_{i,top,} \bullet h_i^{\,2}}{2 \bullet (EI)_{eff,i}} + \frac{V_i \bullet h_i^{\,3}}{3 \bullet (EI)_{eff,i}} \tag{6}$$

where $(EI)_{eff,i}$ is the effective bending stiffness of the CLT panel at the i^{th} storey, and it can be obtained as expressed by Eq. (7).

$$(EI)_{eff,i} = \frac{B_i^{\,3}}{12} \bullet \left[\sum_{k=1}^{n_z} (E_{0,k} \bullet t_{z,k}) + \sum_{k=1}^{n_x} (E_{90,k} \bullet t_{x,k})\right] \tag{7}$$

where $E_{0,k}$ and $t_{z,k}$ are the modulus of elasticity parallel to grain and the thickness of the k^{th} vertical lamination, respectively, $E_{90,k}$ and $t_{x,k}$ are the modulus of elasticity perpendicular to grain and the thickness of the k^{th} horizontal lamination, respectively, and n_z and n_x are the number of laminations along the vertical and horizontal direction, respectively.

2.2.2. *Sliding of shear-wall and displacement between shear-wall and floor panel above*

The inter-storey lateral displacement due to sliding of the shear-wall, $\delta_{A,i}$, can be calculated using Eq. (8).

$$\delta_{A,i} = \frac{V_i}{K_{A,i}} \tag{8}$$

where $K_{A,i}$ is the stiffness of the shear-wall due to sliding, calculated as the product of the lateral shear stiffness, $K_{a,x,i}$, of angle brackets and the number of angle brackets, $n_{a,i}$, namely $K_{A,i} = K_{a,x,i} \bullet n_{a,i}$.

The inter-storey lateral displacement due sliding between the shear-wall under consideration and the floor panel above, $\delta_{F,i}$, can be obtained

from Eq. (9) as follows:

$$\delta_{F,i} = \frac{V_i}{K_{F,i}} \tag{9}$$

where $K_{F,i}$ is the stiffness of the wall due to the floor-to-wall connections, calculated as the product of the lateral-shear stiffness, $K_{f,x,i}$, of a floor-to-wall connection and the number of floor-to-wall connections, $n_{f,i}$, namely $K_{F,i} = K_{f,x,i} \bullet n_{f,i}$.

2.2.3. Rocking deformation

Several proposals have been presented in the literature for the calculation of the inter-storey lateral displacement due to the rocking of a single-panel CLT shear-wall, $\delta_{R,i}$, [13,24,30,35]. In this paper, a modified version of the proposal presented by Gavric et al. [13] is adopted as shown in Eq. (10). Differently from Gavric et al. [13], the length of the contact region between the shear-wall and the ground or the floor below is taken into account in the calculation of the lever arm.

The rocking deformation is expressed as the difference between the inter-storey lateral displacement due to the overturning moment at the base caused by lateral loads, $\delta_{R,M,i}$, and the lateral displacement due to the stabilizing effect of the total vertical load, $\delta_{R,N,i}$. When the stabilizing effect of the vertical loads is greater than the overturning moment caused by lateral loads (i.e., $\delta_{R,M,i} < \delta_{R,N,i}$), the rocking of the shear-wall is prevented and, as a result, the inter-storey lateral displacement due to the rocking kinematic mode, $\delta_{R,i}$, is assumed equal to zero.

$$\delta_{R,i} = \max(\delta_{R,M,i} - \delta_{R,N,i}; 0); \tag{10}$$

The inter-storey lateral displacement due the overturning moment caused by the lateral loads from Eq. (10), $\delta_{R,M,i}$, can be obtained from the product of the inter-storey rotation due to the overturning moment caused by lateral loads, $\varphi_{R,M,i}$, and the inter-storey height, $h_{int,i}$, as expressed in Eq. (11).

$$\delta_{R,M,i} = \varphi_{R,M,i} \bullet h_{int,i} \tag{11}$$

where the inter-storey height is calculated as the sum of the shear-wall height and the floor depth, namely $h_{int,i} = h_i + h_{floor,i}$.

The inter-storey rotation due to the overturning moment caused by the lateral load, $\varphi_{R,M,i}$, is obtained from the ratio of the overturning moment acting at the top of the shear-wall, M_i, and the rocking stiffness of the shear-wall at the i^{th} storey, $K_{R,i}$, as expressed in Eq. (12). The stiffness of the shear-wall due to rocking can be calculated according to Eq. (13) by considering the vertical tensile stiffness of all mechanical anchors that are subjected to uplift (i.e. mechanical anchors that are not within the contact zone).

$$\varphi_{R,M,i} = \frac{M_i}{K_{R,i}} \tag{12}$$

$$K_{R,i} = K_{hd,i} \bullet \left(s_{hd} - b_{c,i}\right)^2 + \sum_{k=1}^{n_{a,z} \le n_a} \left[K_{a,z,k} \bullet \left(s_{a,k} - b_{c,i}\right)^2\right] \tag{13}$$

where $K_{hd,i}$ is the vertical tensile stiffness of the hold-down, $n_{a,z}$ is the number of angle-brackets exhibiting uplift, $K_{a,z,k}$ is the vertical tensile stiffness of the k^{th} angle bracket subjected to uplift, s_{hd} and $s_{a,k}$ are the distance of the hold-down and of the k^{th} angle bracket from the shear-wall end, respectively, and $b_{c,i}$ is the length of the contact region between the shear-wall and the ground or the floor below, as illustrated in Fig. 4.

The value of $b_{c,i}$ can be calculated by considering the deformation contribution related to the contact zone between the panel and the foundation or the floor panel below [36], or alternatively, it can be assumed in the range of $0.05B_i$ and $0.1B_i$[4]

The lateral displacement due to the stabilizing effect of the cumulative vertical load, $\delta_{R,N,i}$, is calculated as the product of the inter-storey rotation due to the vertical load, $\varphi_{R,N,i}$, and the inter-storey height, $h_{int,i}$, according to Eq. (14).

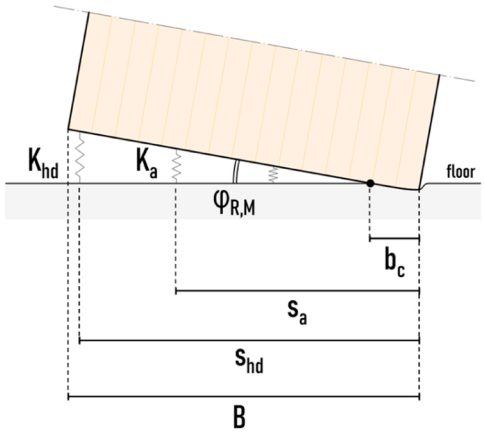

Fig. 4. Rocking kinematic mode of a single-panel shear-wall.

$$\delta_{R,N,i} = \varphi_{R,N,i} \bullet h_{int,i} \tag{14}$$

where the inter-storey rotation $\varphi_{R,N,i}$ can be obtained according to Eq. (15).

$$\varphi_{R,N,i} = \frac{N_i \bullet (0.5B_i - b_{c,i})}{K_{R,i}} \tag{15}$$

The total inter-storey rocking rotation $\varphi_{R,i}$, defined as the ratio between the inter-storey lateral displacement due to the rocking kinematic mode of the wall, $\delta_{R,i}$, and the inter-storey height $h_{int,i}$, can hence be calculated as outlined in Eq. (16).

$$\varphi_{R,i} = \frac{\delta_{R,i}}{h_{int,i}} = \max(\varphi_{R,M,i} - \varphi_{R,N,i}; 0) \tag{16}$$

2.2.4. Rotation of storey below

The inter-storey lateral displacement associated with the rotation of the storey below the wall under consideration, $\delta_{\theta,i}$, can be calculated according to Eq. (17).

$$\delta_{\theta,i} = \theta_{i-1} \bullet h_{int,i} \text{ with } i \ge 1 \tag{17}$$

where θ_{i-1} is the rotation at the top of the shear-wall at the $(i\text{-}1)^{th}$ storey, calculated according to Eq. (18).

$$\theta_{i-1} = \theta_{i-2} + \varphi_{B,i-1} + \varphi_{R,i-1} \tag{18}$$

where θ_{i-2} is the rotation at the top of the shear-wall at the $(i\text{-}2)^{th}$ storey, $\varphi_{B,i-1}$, is the rotation at the top of the shear-wall at the $(i\text{-}1)^{th}$ storey due to the panel bending deformation, as obtained in Eq. (19), and $\varphi_{R,i-1}$ is the rotation at the top of the shear-wall at the $(i\text{-}1)^{th}$ storey due to the rocking, calculated according to Eq. (16), where index i is replaced with index $i\text{-}1$.

$$\varphi_{B,i-1} = \frac{M_{i-1,top,} \bullet h_{i-1}}{(EI)_{eff,i-1}} + \frac{V_{i-1} \bullet h_{i-1}^2}{2 \bullet (EI)_{eff,i-1}} \tag{19}$$

The parameter θ_0 in Eq. 17, when $i = 1$, accounts for the rotation of the substructure below the shear-wall at the ground level and can be assumed equal to zero when the substructure deformation contribution can be neglected.

2.3. Displacement contributions for multi-panel CLT shear-wall

2.3.1. Kinematic modes

Differently from the case involving single-panel CLT shear-walls, only a limited number of proposals are available in the literature for

the analytical prediction of the lateral displacement of multi-panel CLT shear-walls. This behaviour is more complex since it relates to different kinematic rocking modes, which may occur depending on the relative stiffness between the hold-down and the vertical joints. According to Casagrande et al. [5] such kinematic modes include Coupled-Panel (CP), Single-Wall (SW) and Intermediate (IN) kinematic behaviours, as illustrated in Fig. 5.

The CP kinematic mode is observed in cases of relatively stiff hold-down, where each panel is in contact with the ground (or the floor underneath the wall), as shown in Fig. 5(a). The SW kinematic mode occurs in cases, where the hold-down is flexible relative to the vertical joints, and a single centre of rotation is attained for the entire shear-wall (Fig. 5 (c)). The IN kinematic mode contains both CP and SW modes and only some of the panels are in contact with ground (Fig. 5(b)).

The proposed analytical models presented in Casagrande et al. [5] for *m*-panels shear-walls are adopted in this paper to calculate the inter-storey lateral displacement due to the rocking of multi-panel shear-walls composed of *m* panels with the same length *b*.

According to Casagrande et al. [5], if the multi-panel shear-wall is anchored to resist uplift at the corners and the uplift contribution of angle-brackets is neglected, the CP, IN and SW kinematic modes can be obtained when Eqs. (20), (21), and (22), respectively, are satisfied:

$$\frac{K_{\mathrm{hd,i}}}{K_{\mathrm{v,i}}} \geq \frac{1-\widetilde{N}_i \bullet \frac{3m-2}{m^2}}{1-\widetilde{N}_i \bullet \frac{m-2}{m^2}} \quad \text{CP kinematic mode} \tag{20}$$

$$\frac{1-\widetilde{N}_i}{1+\widetilde{N}_i \bullet (m-2)} < \frac{K_{\mathrm{hd,i}}}{K_{\mathrm{v,i}}} < \frac{1-\widetilde{N}_i \bullet \frac{3m-2}{m^2}}{1-\widetilde{N}_i \bullet \frac{m-2}{m^2}} \quad \text{IN kinematic mode} \tag{21}$$

$$\frac{K_{\mathrm{hd,i}}}{K_{\mathrm{v,i}}} \leq \frac{1-\widetilde{N}_i}{1+\widetilde{N}_i \bullet (m-2)} \quad \text{SW kinematic mode} \tag{22}$$

where $K_{hd,i}$ is the vertical tensile stiffness of the hold-down, $K_{\mathrm{v,i}}$ is the shear stiffness of the vertical joint, $\widetilde{N}_i$ is the dimensionless vertical load on the shear-wall at the i^{th} storey, which can be obtained according to Eq. (23).

$$\widetilde{N}_i = \frac{N_i \bullet m \bullet b}{2 \bullet M_i} \tag{23}$$

When the uplift contribution of equally spaced angle-brackets is taken into account, the CP kinematic mode can be attained when the condition expressed in Eq. (24) is satisfied, according to Masroor et al. [21].

$$\frac{K_{\mathrm{hd,i}}}{K_{\mathrm{v,i}}} \geq \frac{1-\frac{\widetilde{N}_i \bullet [3 \bullet m-2]}{m^2}}{\left(1+\frac{\beta \bullet n_a}{2 \bullet m}\right) - \frac{\widetilde{N}_i \bullet \left\{ m \bullet \left(1+\frac{\beta \bullet n_a}{2 \bullet m}\right) - 2 \bullet [1+\alpha \bullet \beta \bullet m] \right\}}{m^2}} \tag{24}$$

where β and α can be obtained using Eqs. (25) and (26), respectively.

$$\beta = \frac{K_{\mathrm{a,z,i}}}{K_{\mathrm{hd,i}}} \tag{25}$$

$$\alpha = \sum_{k=1}^{\frac{n_a}{m}} \left(\frac{k}{\frac{n_a}{m}+1} \right)^2 = \frac{\frac{n_a}{m} \bullet \left(2 \bullet \frac{n_a}{m}+1\right)}{6 \bullet \left(\frac{n_a}{m}+1\right)} \tag{26}$$

Currently, there are no available expressions in literature for the rocking kinematic mode conditions associated with the SW and IN behaviours, when the uplift contribution of angle-brackets is considered.

2.3.2. Panel deformation

The inter-storey lateral displacements due to the panel shear deformation, $\delta_{S,i}$, can be calculated in a similar manner as presented for single-panel shear-walls according to Eq. (3), where B_i is taken as the total length of the shear-wall (i.e., $B_i = m \bullet b_i$). The inter-storey lateral displacement due to panel bending deformation $\delta_{B,i}$, can be calculated using Eq. (6), where $(EI)_{eff,i}$ is the total bending stiffness of the entire multi-panel shear-wall. Similar to composite beams, the total bending stiffness should include the stiffness of the vertical joints between the panels. Such stiffness is expected to range between the value of bending stiffness related to *m* separate panels $(EI)_{0,i}$ and the value related to a single-panel shear-wall $(EI)_{\infty,i}$, with the same total wall length, as expressed by Eqs. (27) to (29). The determination of $(EI)_{\mathrm{eff,i}}$ is a function of several variables, including the elastic modulus, thickness of the wooden lamellae, width of the CLT panels and the stiffness of the vertical joints, and may require engineering judgment depending on the wall configuration and stiffness of the vertical joints between the panels.

$$(EI)_{0,\mathrm{i}} \leq (EI)_{\mathrm{eff,i}} \leq (EI)_{\infty,\mathrm{i}} \tag{27}$$

$$(EI)_{0,i} = m \bullet \frac{b_i^3}{12} \bullet \left[\sum_{k=1}^{n_z} \left(E_{0,\mathrm{k}} \bullet t_{\mathrm{z,k}}\right) + \sum_{k=1}^{n_x} \left(E_{90,\mathrm{k}} \bullet t_{\mathrm{x,k}}\right) \right] \tag{28}$$

$$(EI)_{\infty,i} = \frac{B_i^3}{12} \bullet \left[\sum_{k=1}^{n_z} \left(E_{0,\mathrm{k}} \bullet t_{\mathrm{z,k}}\right) + \sum_{k=1}^{n_x} \left(E_{90,\mathrm{k}} \bullet t_{\mathrm{x,k}}\right) \right] \tag{29}$$

2.3.3. Sliding of shear-wall and displacement between shear-wall and floor panel above

The inter-storey lateral displacements due to the rigid body sliding of the wall, $\delta_{A,i}$, and the sliding between the shear-wall under consideration and the floor panel above, $\delta_{F,i}$, can be calculated with the same approach adopted for a single-panel shear-wall, according to Eqs. (8) and (9).

2.3.4. Rocking and rotation of storey below

The analytical methodologies developed by Casagrande et al. [5] and Masroor et al. [21] are adopted for the calculation of the rotation due to the rocking of the shear-wall, $\varphi_{R,i}$, for CP and SW modes as expressed in Eqs. (30) and (31). Analytical expression for the calculation of the rocking rotation for the IN kinematic mode can be found in Casagrande et al. [5] for the case where the uplift contribution of the angle brackets is neglected. For the SW mode, there are currently no analytical expressions available in literature when the uplift contribution of the angle brackets is considered.

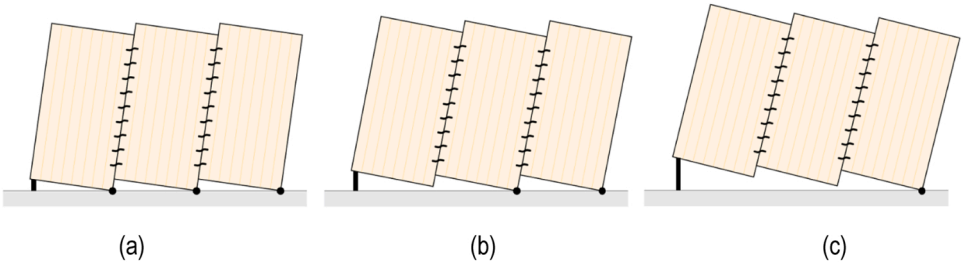

Fig. 5. Kinematic rocking modes for multi-panel CLT shear-wall, CP (a), IN (b) and SW (c).

$$\varphi_{R,i} = \max(\varphi_{R,M,i,CP} - \varphi_{R,N,i,CP}; 0) \text{ for CP mode} \quad (30)$$

$$\varphi_{R,i} = \max(\varphi_{R,M,i,SW} - \varphi_{R,N,i,SW}; 0) \text{ for SW mode} \quad (31)$$

where $\varphi_{R,M,i,CP}$ and $\varphi_{R,M,i,SW}$ are the inter-storey rotation due to the overturning moment caused by lateral loads for the CP and SW mode, respectively (Eqs. (32) and (33)), and $\varphi_{R,N,i,CP}$ and $\varphi_{R,N,i,SW}$ are the inter-storey rotation due the stabilizing effect of the total vertical load for the CP and SW mode, respectively (Eqs. (34) and (35)):

$$\varphi_{R,M,i,CP} = \frac{M_i}{K_{R,i,CP}} \quad (32)$$

$$\varphi_{R,M,i,SW} = \frac{M_i}{K_{R,i,SW}} \quad (33)$$

$$\varphi_{R,N,i,CP} = \frac{N_i \bullet b_i}{2 \bullet K_{R,i,CP}} \quad (34)$$

$$\varphi_{R,N,i,SW} = \frac{N_i}{2 \bullet K_{hd,i} \bullet B_i} \quad (35)$$

$K_{R,i,CP}$ and $K_{R,i,SW}$ represent the rocking stiffness of shear-wall at the i^{th} storey in case of CP and SW kinematic modes, as calculated in accordance with Eqs. (36) and (37), respectively.

$$K_{R,i,CP} = \frac{\left[K_{U,AB} \bullet K_{hd,i} + (m-1) \bullet K_{v,i}\right]}{m^2} \bullet B_i^2 \quad (36)$$

$$K_{R,i,SW} = \left[\frac{1}{K_{hd,i}} + \frac{(m-1)}{K_{v,i}}\right]^{-1} \bullet B_i^2 \quad (37)$$

where $K_{U,AB}$ is the angle-bracket uplift contribution factor. When the uplift contribution of the angle brackets is neglected, this factor is assumed to be equal to unity (i.e., $K_{U,AB} = 1$). When the uplift contribution of angle brackets is considered significant, K_U can be calculated as follows:

$$K_{U,AB} = 1 + \alpha \bullet \beta \bullet m \quad (38)$$

Similar to the case of single-panel CLT shear-walls (Eq. 13), the inter-storey lateral displacement due to the rocking kinematic mode of the wall, $\delta_{R,i}$, can be calculated as provided by Eq. (39).

$$\delta_{R,i} = \max(\varphi_{R,i} \bullet h_{int,i}; 0) \quad (39)$$

As an alternative simplification to the complex expressions presented in Casagrande et al. [5], it is proposed that the inter-storey lateral displacement for the IN kinematic mode be calculated through a linear interpolation between the values calculated assuming CP and SW kinematic mode. The applicability of such approach is discussed in Masroor [22], where the results from analyses on different CLT shear-wall configurations in the IN kinematic mode are conducted and the results from the interpolation are compared to results obtained from the analytical expressions presented by Casagrande et al. [5].

The kinematic modes of the shear-walls may have a significant influence on the inter-storey lateral displacement due to the cumulative rotation of the shear-walls below. These rotations are typically expected to be smaller for CP kinematic mode than SW behaviour but very few studies have addressed this issue in the literature (e.g., [9]). As a result, the same approach adopted for single-panel shear-walls and the same expression for the calculation of the lateral displacement due to the cumulative rotation at the i^{th} storey, $\delta_{\theta,i}$, are considered.

3. Matrix analytical approach

The lateral displacements of LLRSs consisting of multiple shear-walls can be analytically obtained through a matrix formulation as will be discussed in this section. The formulation is first presented for an isolated multi-storey shear-wall and then extended to the case of a LLRS composed of several multi-storey shear-walls placed long the two main directions (x and y) of the building.

3.1. Matrix formulation for isolated multi-storey CLT shear-wall

The analytical methodology outlined in Section 2 for an isolated shear-wall (Fig. 1) is presented in this section through an analytical matrix formulation, as expressed by Eq. (40).

$$\{d_S\} = [K_S]^{-1}\{F_S\} - \{d_{S,N}\} \quad (40)$$

where $\{d_S\}$ is the lateral displacement array, $\{F_S\}$ is the applied lateral load array, $[K_S]$ is the stiffness matrix and $\{d_{S,N}\}$ is the array representing the equivalent lateral displacement due to the vertical loads. The latter represents the reduction in rocking displacement due to the stabilizing effect of the vertical loads as discussed in Section 2.

The stiffness matrix of an isolated multi-storey shear-wall, $[K_S]$, can be obtained as the inverse of the flexibility matrix $[U_S]$ (i.e., $[K_S] = [U_S]^{-1}$), where the generic element, $U_{S,i,j}$, represents the lateral displacement at the i^{th} storey due to a unit lateral force applied at the j^{th} storey of the considered shear-wall.

All contributions related to the vertical load are neglected ($\delta_{R,N,i} = 0; \varphi_{R,N,i} = 0$) in the calculation of $U_{S,i,j}$, since the stabilizing effect due to the vertical load is already included in the term $\{d_{S,N}\}$ of Eq. (40).

In this formulation, an isolated N_s-storey shear-wall with the same inter-storey height h_{int} at all storeys and with a unit lateral load $F_{S,j} = 1$ applied at the j^{th} storey, is considered. The total shear load, V_i, the total overturning moment acting at the bottom, M_i, as well as the total overturning moment acting at the top, $M_{i,top}$, of the i^{th} storey, can be obtained according to Eqs. (41), (42), and (43), respectively.

$$V_i = \begin{cases} 1 & for \quad i \le j \\ 0 & for \quad j < i < N_s \end{cases} \quad (41)$$

$$M_i = \begin{cases} 1 \bullet [j - (i-1)] \bullet h_{int} & for \quad i \le j \\ 0 & for \quad j < i \le N_s \end{cases} \quad (42)$$

$$M_{i,top} = \begin{cases} 1 \bullet (j - i) \bullet h_{int} & for \quad i < j \\ 0 & for \quad j \le i \le N_s \end{cases} \quad (43)$$

The lateral displacement at the i^{th} storey, due to unit lateral force applied at the j^{th} is obtained by summing the contribution of inter-storey displacements to the lateral displacement of the storey below. The procedure is developed starting from the 1st storey and extended to the i^{th} storey.

The lateral displacement, $U_{S,1,j}$, at the first storey (i.e., $i = 1$), due to a unit lateral force applied at the j^{th} storey, can be calculated based on Eq. (2), as presented in Eq. (44).

$$U_{S,1,j} = \delta_{S,1,j} + \delta_{B,1,j} + \delta_{S,1,j} + \delta_{F,1,j} + \delta_{R,M,1,j} + \delta_{\theta,1,j} \quad (44)$$

where $\delta_{\theta,1,j}$ can be assumed to be equal to zero if the rotation of the substructure may be neglected.

For single-panel CLT shear-walls, by substituting Eqs. (3), (6), (8), (9), (10), (11) and (12) into Eq. (44), one obtains:

$$U_{S,1,j} = \frac{h}{G_{eff,1} \bullet t_{CLT,1} \bullet B_1} + \left[\frac{(j-1) \bullet h_{int} \bullet h^2}{2 \bullet (EI)_{eff,1}} + \frac{h^3}{3 \bullet (EI)_{eff,1}}\right] + \frac{1}{K_{A,1}} + \frac{1}{K_{F,1}} + \frac{j \bullet h_{int}}{K_{R,1}} \bullet h_{int} \quad (45)$$

The equivalent displacement due to the vertical loads at the 1st storey, $d_{S,N,1}$, can be calculated according to Eq. (46) by considering the inter-storey rocking due to vertical load, based on Eqs. (14) and (15).

$$d_{S,N,1} = \varphi_{R,N,1} \bullet h_{\text{int}} = \frac{N_1 \bullet (0.5B_1 - b_{c,1})}{K_{R,1}} \bullet h_{\text{int}} \tag{46}$$

Similarly, the lateral displacement at the 2nd storey, due to unit lateral force applied at the j^{th} storey, $U_{S,2,j}$, can be expressed as:

$$U_{S,2,j} = U_{S,1,j} + \delta_{S,2,j} + \delta_{B,2,j} + \delta_{S,2,j} + \delta_{F,2,j} + \delta_{R,M,2,j} + \delta_{0,2,j} \tag{47}$$

Substituting Eqs. (3), (6), (8), (9), (10), (11) and (12) into Eq. (47), one obtains:

$$U_{S,2,j} = U_{S,1j} + \frac{h}{G_{eff,2} \bullet t_{\text{CLT},2} \bullet B_2} + \left[\frac{(j-2)\bullet h_{\text{int}} \bullet h^2}{2 \bullet (EI)_{eff,2}} + \frac{h^3}{3 \bullet (EI)_{eff,2}}\right] + \frac{1}{K_{A,2}} + \frac{1}{K_{F,2}} + \frac{(j-1) \bullet h_{\text{int}}}{K_{R,2}} \bullet h_{\text{int}} + \theta_{1,j} \bullet h_{\text{int}} \tag{48}$$

where $\theta_{1,j}$ is calculated according to Eqs. (18) and (19), as presented in Eq. (49).

$$\theta_{1,j} = \theta_0 + \varphi_{B,1,\text{j}} + \varphi_{R,\text{M},1,\text{j}} = 0 + \frac{(\text{j}-1)\bullet h_{\text{int}} \bullet h}{(EI)_{eff,1}} + \frac{h^2}{2 \bullet (EI)_{eff,1}} + \frac{j \bullet h_{\text{int}}}{K_{R,1}} \tag{49}$$

Substituting Eq. (49) into Eq. (48), $U_{S,2,j}$ can be calculated as:

$$U_{S,2,j} = U_{S,1j} + \frac{h}{G_{eff,2} \bullet t_{\text{CLT},2} \bullet B_2} + \left[\frac{(j-2)\bullet h_{\text{int}} \bullet h^2}{2 \bullet (EI)_{eff,2}} + \frac{h^3}{3 \bullet (EI)_{eff,2}}\right] + \frac{1}{K_{A,2}} + \frac{1}{K_{F,2}} + \frac{(j-1) \bullet h_{\text{int}}}{K_{R,2}} \bullet h_{\text{int}} + \left(\frac{(j-1) \bullet h_{\text{int}} \bullet h}{(EI)_{eff,1}} + \frac{h^2}{2 \bullet (EI)_{eff,1}} + \frac{j \bullet h_{\text{int}}}{K_{R,1}}\right) \bullet h_{\text{int}} \tag{50}$$

The rotation at the top of the 2nd storey $\theta_{2,j}$ is calculated according to Eqs. (18) and (19) as expressed by Eq. (51):

$$\theta_{2,j} = \theta_{1,j} + \varphi_{B,2,\text{j}} + \varphi_{R,M,2,\text{j}} = \theta_{1,j} + \frac{(j-2) \bullet h_{\text{int}} \bullet h}{(EI)_{eff,2}} + \frac{h^2}{2 \bullet (EI)_{eff,2}} + \frac{(j-1) \bullet h_{\text{int}}}{K_{R,2}} \tag{51}$$

The displacement due to the vertical loads, $d_{S,N,2}$, can be calculated by considering the rocking displacement, $d_{S,N,1}$, and the rocking rotation of the shear-wall at the storey below, $\varphi_{R,N,1}$, due to the vertical loads, as expressed in Eq. (52).

$$d_{S,N,2} = d_{S,N,1} + (\varphi_{R,N,1} + \varphi_{R,N,2}) \bullet h_{\text{int}} = d_{S,N,1} + \left(\frac{N_1 \bullet (0.5B_1 - b_{c,1})}{K_{R,1}} + \frac{N_2 \bullet (0.5B_2 - b_{c,2})}{K_{R,2}}\right) \bullet h_{\text{int}} \tag{52}$$

At the i^{th} storey, where $i \le j$, Eqs. (50) and (51) can be generalized as expressed by Eqs. (53) and (54), respectively.

$$U_{S,i,j} = U_{S,i-1,j} + \frac{h}{G_{eff,i} \bullet t_{\text{CLT,i}} \bullet B_i} + \left[\frac{(j-i)\bullet h_{\text{int}} \bullet h^2}{2 \bullet (EI)_{eff,i}} + \frac{h^3}{3 \bullet (EI)_{eff,i}}\right] + \frac{1}{K_{A,i}} + \frac{1}{K_{F,i}} + \frac{(j-i+1) \bullet h_{\text{int}}}{K_{R,i}} \bullet h_{\text{int}} + \theta_{i-1} \bullet h_{\text{int}} \tag{53}$$

$$\theta_{i,j} = \theta_{i-1,j} + \varphi_{B,i,j} + \varphi_{R,M,i,j} = \theta_{i-1,j} + \frac{(j-i) \bullet h_{\text{int}} \bullet h}{(EI)_{eff,i}} + \frac{h^2}{2 \bullet (EI)_{eff,i}} + \frac{(j-i+1) \bullet h_{\text{int}}}{K_{R,i}} \tag{54}$$

Alternatively, for the i^{th} storey, where $j < i \le N_s$, since the shear and bending moment are equal to zero, $U_{S,i,j}$ and $\theta_{i,j}$ can be obtained as expressed in Eqs. (55) and (56), respectively:

$$U_{S,i,j} = U_{S,j,j} + \theta_{j,j} \bullet (i-j) \bullet h_{\text{int}} \tag{55}$$

$$\theta_{i,j} = \theta_{j,j} \tag{56}$$

The generic element $U_{S,i,j}$ of the flexibility matrix $[U_S]$ can hence be expressed as:

$$U_{S,i,j} = \begin{cases} U_{S,i-1,j} + \dfrac{h}{G_{eff,i} \bullet t_{\text{CLT,i}} \bullet B_i} + \left(\dfrac{(j-i)\bullet h_{\text{int}} \bullet h^2}{2 \bullet (EI)_{eff,i}} + \dfrac{h^3}{3 \bullet (EI)_{eff,i}}\right) + \dfrac{1}{K_{A,i}} + \dfrac{1}{K_{F,i}} + \dfrac{(j-i+1) \bullet h_{\text{int}}}{K_{R,i}} \bullet h_{\text{int}} + \theta_{i-1,j} \bullet h_{\text{int}} & \text{for} \quad i \le j \\ U_{S,j,j} + \theta_{j,j} \bullet (i-j) \bullet h_{\text{int}} & \text{for} \quad j < i \le N_s \end{cases} \tag{57}$$

The displacement due to the vertical loads, $d_{S,N,i}$ can be generalized as expressed in Eq. (58).

$$d_{S,N,i} = d_{S,N,i-1} + \sum_{r=1}^{i} \varphi_{R,N,\text{r}} \bullet h_{\text{int}} = d_{S,N,i-1} + \sum_{r=1}^{i} \frac{N_r \bullet (0.5B_r - b_{c,r})}{K_{R,r}} \bullet h_{\text{int}} \tag{58}$$

The same procedure presented in this section for the case of a single-panel CLT shear-wall can be extended to the case of multi-panel CLT shear-walls by considering the expressions reported in Section 2.2.

3.2. Matrix formulation for the LLRS

The analytical methodology outlined in the previous section for an isolated shear-wall is extended to the LLRS composed of shear-walls along the x and y directions (Fig. 6). The out-of-plane bending stiffness of the floor as well as any interaction between floors and walls are neglected.

In the formulation presented in this study, a diaphragm constrain is assumed to connect the shear-walls together at each storey level in order to simulate the effect of a rigid diaphragm. It is noteworthy to mention that, for CLT buildings, the assumption of rigid diaphragm should be validated for the given design and should not always be taken for granted. Despite the fact that a reasonable number of research studies have been conducted in past years, aimed at investigating the in-plane behaviour of CLT floors [17–19,23], differently from other materials (e.g. reinforced concrete), limited prescriptive requirements regarding the rigidity of floor diaphragms have been developed and adopted in Standards. It is generally agreed, however, that in order to ensure adequate in-plane stiffness of CLT floors, panel-to-panel connection should be designed with sufficient overstrength and large openings and discontinuities should be adequately reinforced.

A Cartesian coordinate system is located at the ground floor and the intersection of z-axis with the floors at the i^{th} storey is represented by

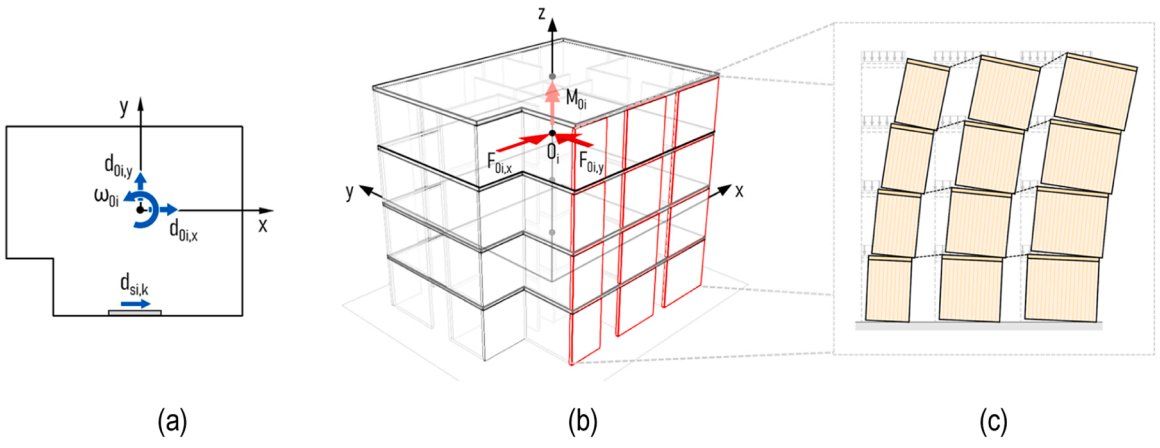

Fig. 6. Shear-wall line as part of the Lateral Load Resisting System. a) lateral displacement components of the ith floor; 2) lateral loads applied at the ith floor; 3) deformed shape of the lateral load resisting system.

point O_i, as shown in Fig. 6a. Due to the inclusion of the rigid diaphragm behaviour, the kinematic behaviour of the LLRS can be expressed by an array of lateral displacements $\{d_{LLRS}\}$ of dimensions $3N_s \times 1$, according to Eq. (59).

$$\{d_{LLRS}\} = \left\{ d_{O_1,x}, d_{O_1,y}, \omega_{O_1}, \ldots\ldots, d_{O_i,x}, d_{O_i,y}, \omega_{O_i}, \ldots\ldots, d_{O_{N_s},x}, d_{O_{N_s},y}, \omega_{O_{N_s}} \right\}^T \tag{59}$$

where $d_{O_i,x}$ and $d_{O_i,y}$ are the lateral displacements of point O_i along the x- and y-direction, respectively, and ω_{O_i} is the rotation of point O_i at the i^{th} storey.

The array of lateral loads $\{F_{LLRS}\}$ acting on the LLRS are of dimensions $3N_s \times 1$, and they can be expressed according to Eq. (60), see Fig. 6b.

$$\{F_{LLRS}\} = \left\{ F_{O_1,x}, F_{O_1,y}, M_{O_1}, \ldots\ldots, F_{O_i,x}, F_{O_i,y}, M_{O_i}, \ldots\ldots, F_{O_{N_s},x}, F_{O_{N_s},y}, M_{O_{N_s}} \right\}^T \tag{60}$$

where $F_{O_i,x}$ and $F_{O_i,y}$ are the lateral loads applied at point O_i along the x- and y-direction at the i^{th} storey, respectively, and M_{O_i} is the torsional moment applied at point O_i at the i^{th} storey.

The matrix formulation for the generic k^{th} isolated shear-wall can be written by rearranging Eq. (40), as expressed in Eq. (61):

$$\{F_S\}_k = [K_S]_k \left(\{d_S\}_k + \{d_{S,N}\}_k \right) \tag{61}$$

where $\{d_S\}_k$ represent the lateral displacement of the isolated j^{th} shear-wall (Fig. 6c), and $\{F_S\}_j$ represents the array of lateral loads applied by the diaphragm at each storey on the k^{th} shear-wall.

Due to the assumed in-plane rigidity of the floor, the lateral displacement array for the kth shear-wall, $\{d_S\}_k$, can be related to the array of the lateral displacement of the LLRS, $\{d_{LLRS}\}$, according to Eq. (62):

$$\{d_S\}_k = [C_S]_k \{d_{LLRS}\} \tag{62}$$

where $[C_S]_k$ is an $N_s \times 3N_s$matrix that associates the displacement of the k^{th} shear-wall to the displacements of the reference point O_i, as a function of the orientation of the shear-wall and distance from the point O_i. Substituting Eq. (62) in Eq. (61), one obtains:

$$\{F_S\}_k = [K_S]_k \left([C_S]_k \{d_{LLRS}\} + \{d_{S,N}\}_k \right) \tag{63}$$

From the principle of virtual work, the work done by the LLRS is set equal to the sum of works done by each shear-wall, as expressed by Eq. (64):

$$\{F_{LLRS}\} \bullet \delta\{d_{LLRS}\} = \sum \{F_S\}_k \bullet \delta\{d_S\}_k \tag{64}$$

where δ represent the infinitesimal variation of the displacement arrays.

Substituting Eqs. (62) and (63) into Eq. (64), one obtains Eq. (65). This equation can be simplified as shown in Eq. (66) and rewritten as shown in Eq. (67).

$$\{F_{LLRS}\} \bullet \delta\{d_{LLRS}\} = \sum [K_S]_k \left([C_S]_k \{d_{LLRS}\} + \{d_{S,N}\}_k \right) \bullet [C_S]_k \delta\{d_{LLRS}\} \tag{65}$$

$$\{F_{LLRS}\} = \left(\sum [C_S]_k{}^T [K_S]_k [C_S]_k \right) \bullet \{d_{LLRS}\} + \sum [C_S]_k{}^T [K_S]_k \{d_{S,N}\}_k \tag{66}$$

$$\{F_{LLRS}\} = [K_{LLRS}]\{d_{LLRS}\} + \{F_{LLRS,N}\} \tag{67}$$

where $[K_{LLRS}]$ is the LLRS stiffness matrix and $\{F_{LLRS,N}\}$ is the LLRS equivalent lateral force array related to the vertical loads, which can be obtained as presented in Eqs. (68) and (69), respectively:

$$[K_{LLRS}] = \sum [C_S]_k{}^T [K_S]_k [C_S]_k \tag{68}$$

$$\{F_{LLRS,N}\} = \sum [C_S]_k{}^T [K_S]_k \{d_{S,N}\}_k \tag{69}$$

By rearranging Eq. (67), the lateral displacements of the LLRS can be calculated as expressed in Eq. (70):

$$\{d_{LLRS}\} = [K_{LLRS}]^{-1} \cdot \left(\{F_{LLRS}\} - \{F_{LLRS,N}\} \right) \tag{70}$$

3.3. Rocking displacement consistency

The lateral displacements obtained from Eq. (70) may not be consistent with the initial conditions assumed for the system, where rocking is assumed to occur in each shear-wall and at each storey. This condition may not be satisfied when the overturning moment is lower than the stabilizing moment due to the vertical loads. A verification on the rocking displacement consistency is therefore needed.

Knowing the lateral displacements from Eq. (70), the lateral force array acting on each isolated shear-wall, $\{F_S\}_k$, can be calculated according to Eqs. (61) and (62) from which the overturning moment action at the bottom of the i^{th} storey, $M_{i,k}$, can be calculated as expressed by Eq. (71).

$$M_{i,k} = \sum_{r=i}^{n} F_{S,r,k} \cdot (r - i + 1) \cdot h_{int} \tag{71}$$

The stabilizing moment of the k^{th} single- and multi-panel shear-wall can be calculated using Eqs. (72) and (73), respectively.

$$M_{\mathrm{stab,i,k}} = N_{i,k} \cdot \frac{B}{2} \quad \text{for single} - \text{panel shear} - \text{wall} \tag{72}$$

$$M_{\mathrm{stab,i,k}} = N_{i,k} \cdot \frac{b}{2} \quad \text{for multi} - \text{panel shear} - \text{wall} \tag{73}$$

The condition for the activation of the rocking mechanism at the i^{th} storey of the k^{th} shear-wall can be expressed as reported in Eq. (74).

$$\Delta M_{\mathrm{i,k}} = |M_{\mathrm{i,k}}| - |M_{\mathrm{stab,i,k}}| \tag{74}$$

If $\Delta M_{\mathrm{i,k}} > 0$, the rocking mechanism is activated as assumed in the initial condition of the analysis. If $\Delta M_{\mathrm{i,k}} < 0$, the rocking mechanism is not activated and the LLRS should be reanalyzed. This implies that the stiffness matrix and the vertical load array of the k^{th} shear-wall have to be recalculated by assuming that the rocking deformation contribution at the i^{th} storey is neglected, namely $K_{\mathrm{R,i,k}} \rightarrow \infty$. The procedure to follow in this case involves recalculating the lateral displacements according to Eq. (70), where the updated stiffness matrix and vertical load array are adopted. The lateral force array acting on each isolated shear-wall can hence be recalculated according to Eqs. (61) and (62) from which the new values of overturning moment action at the bottom of the ith storey can be determined as expressed by Eq. (71). If the new values of the overturning moments are greater than the corresponding stabilizing moments, the rocking displacement consistency is satisfied. Otherwise, a new iteration of the process is required.

A similar procedure has to be adopted in the case of multi-panel shear-walls to verify the consistency in terms of kinematic modes. The analysis is conducted by assuming CP or SW kinematic mode of the k^{th} shear-wall at the i^{th} storey. This assumption has to be verified by the kinematic mode conditions reported in Section 2.3.

4. Experimental validation of the proposed analytical approach

The validation of the proposed analytical approach was conducted by comparing the displacements obtained from the analytical expressions presented in the previous section with those obtained from experimental tests on twelve single-storey shear-walls and one two-storey shear-wall available in the literature ([13], [8], [26], and [27]).

Both single- and multi-panel shear-walls, subjected to monotonic or cyclic loading were considered. The single-storey shear-walls had heights between 2.30 and 2.95 m and lengths between 1.25 and 2.95 m whereas the two-storey shear-wall tested by Popovski et al. [27] consisted of two 2.3 m x 2.3 m CLT vertical panels interlayered by a horizontal 94 mm thick CLT slab. All shear-walls had thicknesses between 85 and 100 mm, and were constructed using 3- or 5-layer CLT panels.

The majority of the test specimens consisted of shear-walls with traditional hold-down and angle-bracket mechanical anchors fastened with annular ringed nails 4 × 60 mm, and anchored to steel beams representing the foundation through bolts with diameter between 8 and 12 mm. The exception to this was the tests conducted by D'Arenzo et al. [8] and Popovski et al. [27] in which only angle-brackets were used to limit both rocking and sliding of the walls, the wall tests conducted by Polastri and Casagrande [26], where the sliding mechanism was prevented through shear keys, and the tests performed by Popovski et al. [27] on single-storey shear-walls, in which spiral nails 3.9 × 89 mm were used. The connection typologies adopted for the vertical joints of the segmented walls included half-lap joints and spline joints with partially threaded screws, and shear keys with rigid connectors. In the two-storey shear-wall, the floor was connected to the wall by means of 8 × 200 mm screws with 200 mm spacing. The geometrical and mechanical properties of the tested shear-walls used for the validation of the analytical expressions are reported in the Supplementary Material using the symbol naming convention used in the previous sections.

Figs. 7, 8 and 9 show the comparison between the load-displacement

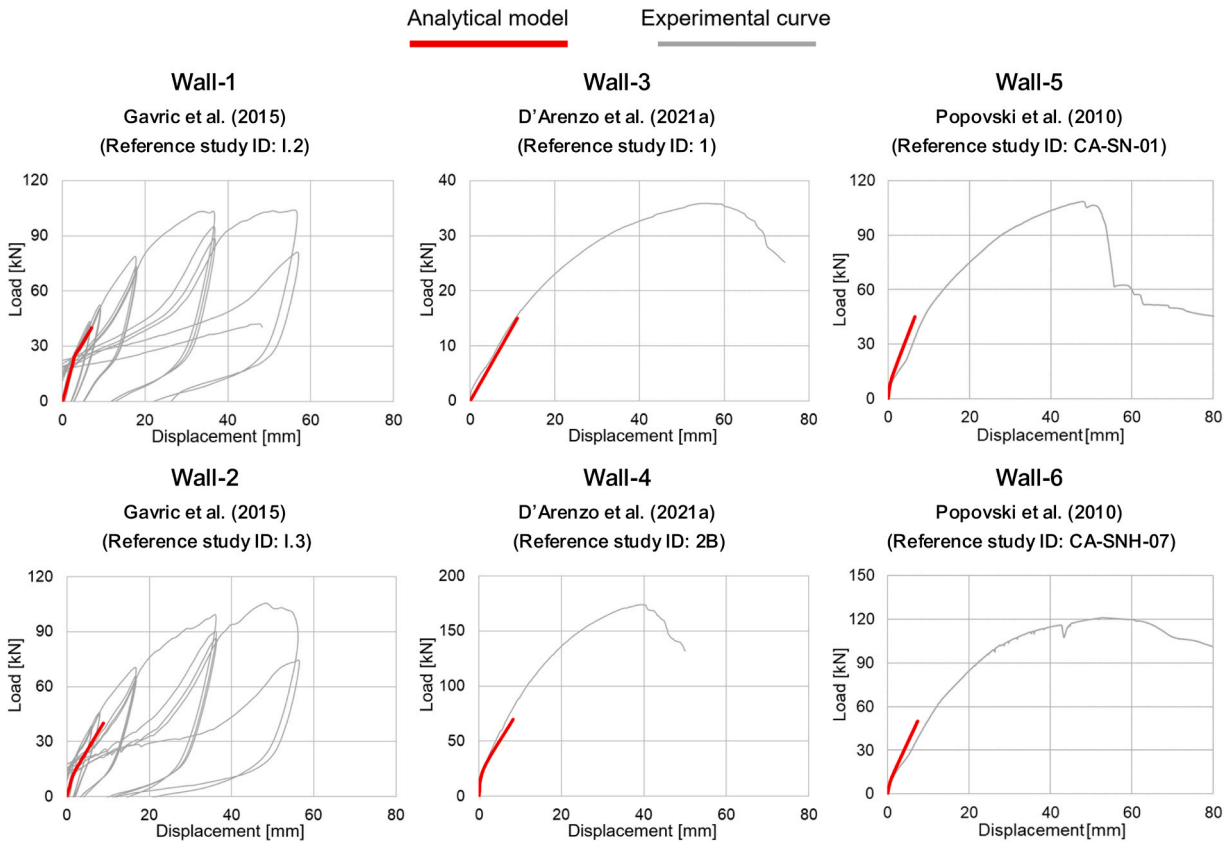

Fig. 7. Validation of the proposed analytical approach for single-panel single-storey shear-walls.

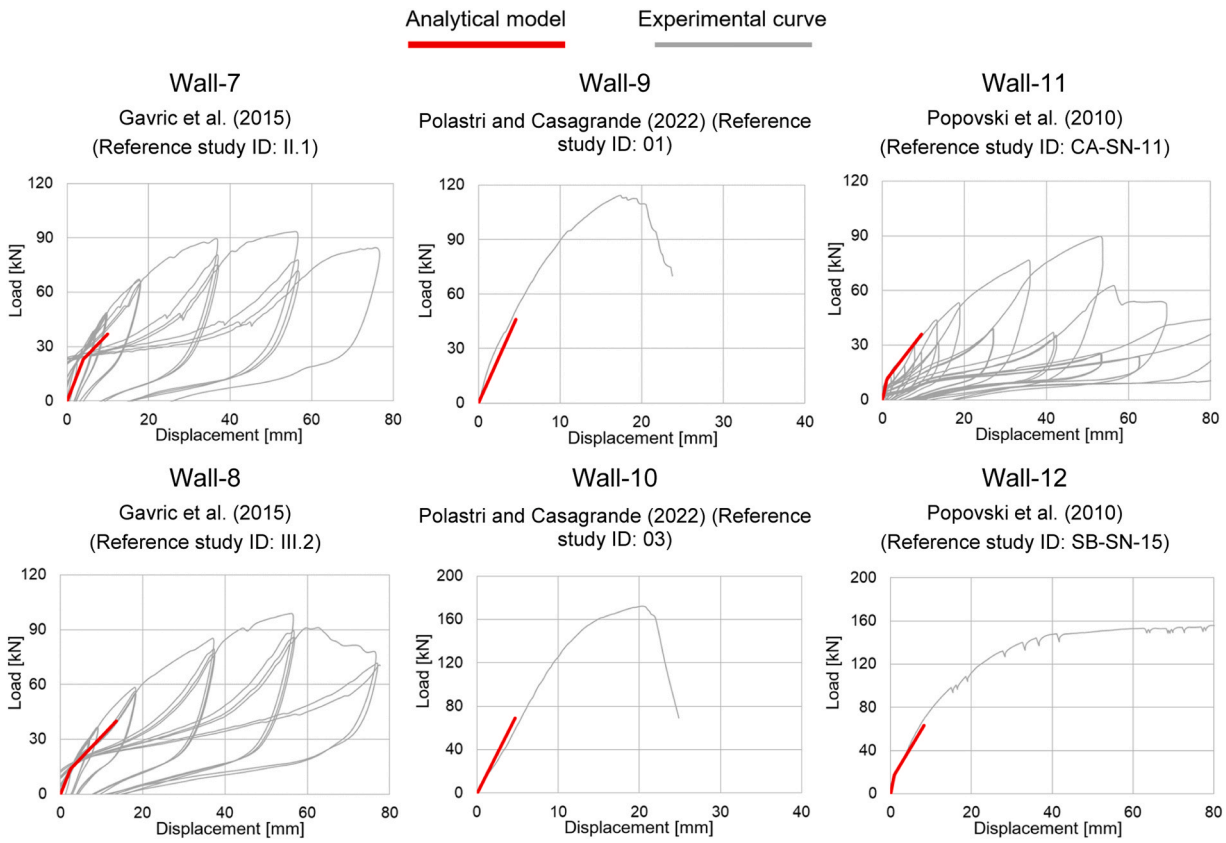

Fig. 8. Validation of the proposed analytical approach for multi-panel single-storey shear-walls.

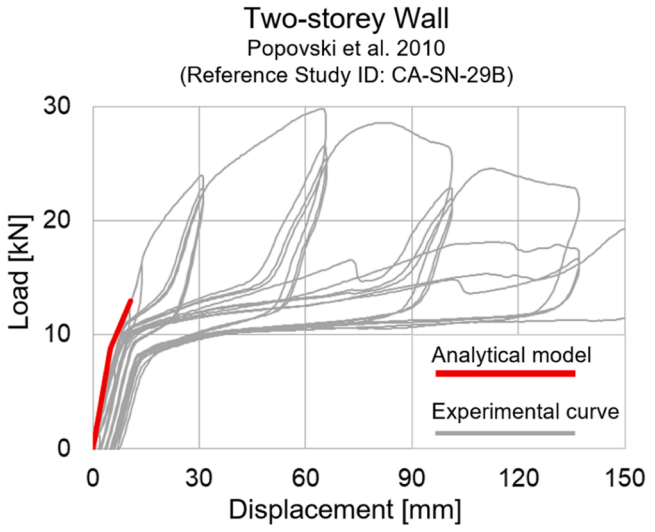

Fig. 9. Validation of the proposed analytical approach for the two-storey shear-wall.

curves obtained from the experimental tests and the proposed expressions, with nomenclature adopted in the original study (in bracket) and in the current study. The curve for the proposed deflection equation was limited to 40% of the maximum load since the predictive model's capability is limited to the elastic range. The graphs show a good agreement between the experimental and analytical load displacement curves, highlighting the ability of the proposed model to predict the elastic response of both single- and multi-panel CLT shear-walls.

5. Verification of the proposed analytical matrix approach against numerical modelling - case study

In this section two design examples serve to verify the proposed procedure against numerical modelling. These examples aim to demonstrate that the developed expressions are mathematically accurate. The first example includes a two-storey LLRS composed of two parallel single-panel CLT shear-walls, while the second example is used to verify the expressions for the lateral displacements for a three-storey two-panel shear-wall, as illustrated in Fig. 10.

5.1. Single-panel CLT shear-walls

A two-storey LLRS composed of two parallel single-panel CLT shear-walls of length B equal to 5.0 m (Wall 1) and 2.5 m (Wall 2) is analysed. The height of the walls, h, at both storeys is assumed to be equal to 2.5 m, and the depth of the floor h_{floor} is taken equal to 0.2 m. The inter-storey height h_{int} is hence equal to 2.7 m in both storeys.

5-ply CLT panels with thickness, t_{CLT}, equal to 100 mm (i.e., 20 mm equal layer thickness) are adopted for all walls. The CLT panels are manufactured using laminations with width, w, equal to 150 mm, modulus of elasticity parallel to the grain, E_0, equal to 12,000 MPa and an in-plane shear modulus, G_0, equal to 690 MPa. A hold-down characterized by a vertical tensile stiffness, K_{hd}, equal to 15,000 kN/m is placed at both ends of the walls at the first storey, whereas a hold-down with stiffness equal to 10,000 kN/m is adopted at the two ends of the walls at the second storey. Four angle brackets with lateral shear stiffness, $K_{a,x}$, equal to 10,000 kN/m are used at both storeys of Wall 1. Two angle brackets with same stiffness of those adopted in Wall 1 were used at both storeys of Wall 2. A vertical tensile stiffness of the angle brackets, $K_{a,z}$, equal to 3000 kN/m is assumed. The floor-to-wall connections for both floors consist of twenty 10 × 300 mm screws uniformly distributed along Wall 1 and ten 10 × 300 mm screws uniformly distributed along

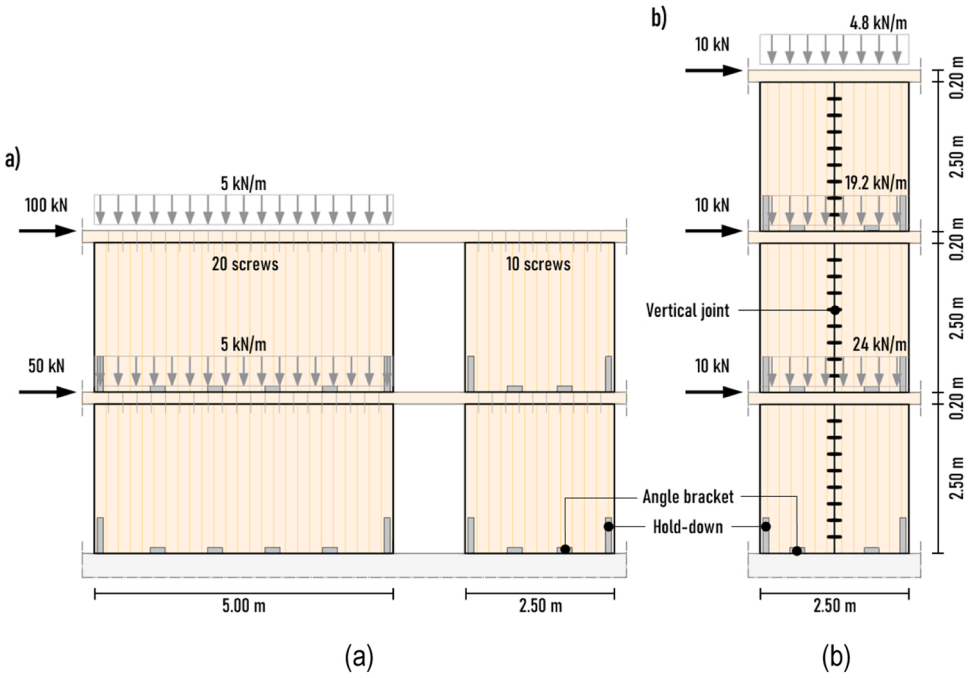

Fig. 10. Design examples: (a) two-storey with two parallel single-panel CLT shear-walls, (b) 3-storey two-panel shear-wall.

Wall 2. Each screw is characterized by a lateral shear stiffness, $K_{f,x}$, equal to 1000 kN/m.

A lateral load equal to 50 kN and 100 kN is applied on the LLRS at the first and second storey, respectively. The array of the lateral loads $\{F_{LLRS}\}$ acting on the LLRS, can hence be expressed according to Eq. (75). It is noteworthy to mention that since a 2D LLRS is considered in this example, only the components of lateral loads in the plane of the walls are considered, neglecting the load components in the out-of-plane direction as well as the torsional moment.

$$\{F_{LLRS}\} = \{F_{O_1}, F_{O_2}\}^T = \begin{Bmatrix} 50 \\ 100 \end{Bmatrix} \bullet 10^3 \quad N \tag{75}$$

A gravity load equal to 5 kN/m is applied at both storeys of Wall 1, while Wall 2 is considered to have zero gravity load.

The lateral displacements and lateral forces of each wall are calculated according to procedure reported in the previous sections and are expressed in Eqs. (76) to (78). Detailed calculations are reported in the Supplementary Material.

$$\{d_S\}_{Wall1} = \{d_S\}_{Wall2} = \begin{Bmatrix} 12.4 \\ 24.3 \end{Bmatrix} mm \tag{76}$$

$$\{F_S\}_{Wall1} = \begin{Bmatrix} 2.9 \\ 8.0 \end{Bmatrix} \bullet 10^4 N \tag{77}$$

$$\{F_S\}_{Wall2} = \begin{Bmatrix} 2.1 \\ 2.0 \end{Bmatrix} \bullet 10^4 N \tag{78}$$

A verification of the equations developed in the current study against numerical modelling is presented using SAP2000 software [7], employing the mechanical properties of connections and CLT panels presented earlier, in order to demonstrate their mathematical accuracy. Fig. 11 illustrates the numerical model developed for this system. The connections were modelled by using link elements that represent their stiffness. Angle brackets were considered in both uplift and shear, while hold-downs were assumed to act only in uplift. To simulate contact between the CLT panels and the foundation below, gap elements with a

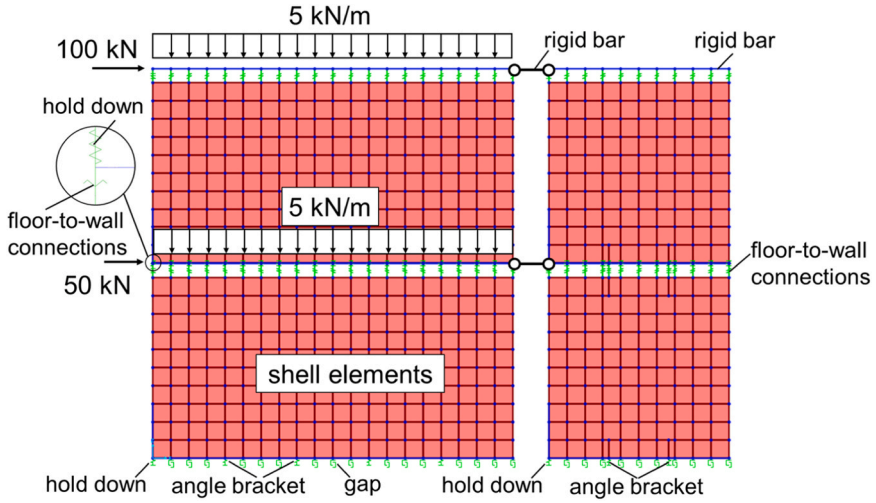

Fig. 11. The LLRS system composed of two CLT shear-walls modelled in SAP2000.

Table 1
The results obtained from the developed equations and numerical models.

Parameter	Analytical models	Numerical models	Discrepancy
$d_{S,1}$ (mm)	12.4	11.5	7.7%
$d_{S,2}$ (mm)	24.3	22.2	9.5%
$F_{S,1,1}$ (kN)	29.3	29.1	0.8%
$F_{S,2,1}$ (kN)	80.4	79.7	0.9%
$F_{S,1,2}$ (kN)	20.8	20.9	0.7%
$F_{S,2,2}$ (kN)	19.6	20.3	3.3%

high compression stiffness of 10^8 kN/m and no tension stiffness were used. Gap elements were also used to simulate the contact between the CLT panels and the floor below. However, in this case the deformability of the CLT floor in the direction perpendicular to the grain of the external layers was considered following the modelling strategy employed by D'Arenzo et al. [8]. This approach led to a compression stiffness of 175.000 kN/m, having considered a distance between the gap elements of 250 mm and a modulus of elasticity perpendicular to the grain of 600 MPa. The floors were modelled using rigid bars placed 200 mm from the top of the shear-walls. The top of the walls at the first and second storeys were connected to the rigid bars with multi-linear link elements acting only horizontally in order to simulate the floor-to-wall connection. The bottom of the walls at the first and second storeys were attached to the ground and the floor at the first storey, respectively, by means of link elements representing hold-down, angle brackets, and gap elements.

Diaphragm constraints were applied to the points of the rigid bars representing the floors at the first and second storeys to simulate diaphragm floor behaviour. Horizontal and vertical loads were applied on the rigid bar elements representing the floor.

Table 1 presents the lateral displacement and distributed loads at the first and second storey floors obtained from the analytical and numerical models. The discrepancies between the two methods are within an acceptable range, with a maximum difference of 9.8% in the lateral displacements, and 3.3% in distributed forces. The observed discrepancies could be attributed to the compression zone used in the analytical solution, assumed to be 10% of the length of the walls. The compression zone length could be smaller as the magnitude of gravity loads for Wall 1 and 2 were not very significant. Additional analytical calculations were conducted on the same example while ignoring the compression zone (i.e. $b_C = 0$), and a maximum difference of 0.8% was observed between both lateral displacements and distributed forces. This demonstrates the high accuracy of the developed equations.

5.2. Multi-panel CLT shear-wall

A three-storey two-panel CLT shear-wall of total length B equal to 2.5 m (individual panel's length equal to 1.25 m) is analysed. The height of the walls, h, is assumed to be equal to 2.5 m for all three storeys. The same CLT panels used for the example reported in Section 6.1 are used in this example. Hold-downs with a vertical tensile stiffness, $K_{hd,i}$, equal to 15,000 kN/m, 10,000 kN/m and 5000 kN/m were placed at both ends of the walls at the first, second and third storey, respectively. In all storeys, two angle brackets with lateral shear stiffness, $K_{a,x}$, equal to 10,000 kN/m are used. The vertical tensile stiffness of the angle brackets was ignored since closed-form equations are not developed for SW when the uplift contribution of angle brackets is included. The vertical joint consists of ten joints, each with a shear stiffness of 2000 kN/m, resulting in a total shear stiffness of the vertical joint of 20,000 kN/m. A rigid floor-to-wall connection along the shear horizontal direction was assumed at each storey. A lateral load equal to 10 kN is applied on the LLRS at each storey. Uniformly distributed gravity loads equal to 24 kN/m, 19.2 kN/m, and 4.8 kN/m were applied on top of first, second, and third storeys, respectively.

A numerical model implemented in SAP2000 software [7] was developed (Fig. 11 (a)) to demonstrate the mathematical accuracy of the equations proposed in the current study. All connections were modelled using multi-linear link elements. To simulate contact between the CLT panels and the foundation below, gap elements with a high compression stiffness of 10^8 kN/m and no tension stiffness were used. Also in this case, gap elements were used to simulate the contact between the CLT panels and the floor below taking into account the deformability of the CLT floor in the direction perpendicular to the grain of the external layers, following the modelling approach presented by D'Arenzo et al. (2021a). This approach led to a compression stiffness of 175.000 kN/m, having considered a distance between the gap elements of 250 mm and a modulus of elasticity perpendicular to the grain of 600 MPa. The floors were modelled in a similar way to that described in Section 5.1. Diaphragm constraints were applied to top points of each shearwall at each storey to simulate diaphragm floor behaviour. The link elements representing the floor-to-wall connections were assumed to be fully flexible along the vertical direction in order to allow the relative rotation of the panels and to avoid floor-wall interaction. At each storey, a rotational rigid-body constraint was also applied between the rigid bar and the outermost panel farthest away from the load application point in order to transmit the wall rotation to the floor above.

Horizontal concentrated forces were applied to the rigid bar representing the floor. Since the link elements connecting the floor to the wall below are flexible in the vertical direction, they are not able to transmit the vertical load from the rigid bar to the wall below. As a result, a vertical load equivalent to the total load on that storey is applied at the top of the wall panels at each storey, while a load with the same magnitude but in opposite direction is applied to the rigid bar below. This allows the vertical gravity load at the top of the wall panels to contribute to the stabilizing effect while the vertical load applied at the rigid bar below only ensures that the gravity load is not transmitted between storeys. The application of total vertical load rather than storey loads at each storey level ensures that the force transfer between storeys is maintained correctly. This procedure is illustrated as way of example for the wall of the second storey in Fig. 12 (a).

As illustrated in Fig. 12 (b), the rocking kinematic mode achieved at each storey was CP for the first and second storeys and SW for the third storey. Table 2 summarizes the lateral displacement at the top of each storey, obtained from the numerical model and the proposed equations. Although the kinematic modes at each storey differed, the analytical model was able to accurately predict the lateral displacement at each level with less than 0.5% discrepancy.

6. Conclusions

This paper presents an analytical approach for the calculation of the elastic lateral displacements of multi-storey platform-type CLT shear-walls in both single-panel and multi-panel configuration. Analytical formulas for the calculation of the in-plane bending and shear panel displacement, sliding, rocking, floor-to-wall displacements and cumulative rotational displacements based on the elastic properties of CLT panels and wall base connections are provided for single- and multi-panel multi-storey CLT shear-walls.

The proposed analytical method was validated against twelve single- and multi-panel experimental CLT shear-wall tests conducted in four previous independent experimental campaigns. The analytical-experimental comparison confirmed the suitability of the proposed model to predict the elastic lateral displacement response for both single- and multi-panel CLT shear-walls.

The proposed analytical expressions for the elastic lateral displacement calculation of an isolated CLT shear-wall was further expanded to the case of a LLRS composed of several multi-storey CLT shear-walls through a matrix formulation. A verification of the proposed analytical matrix approach was performed against numerical models representing two-storey consisting of single-panel shear-walls and a three-storey two-panel CLT shear-wall. The comparison was performed in

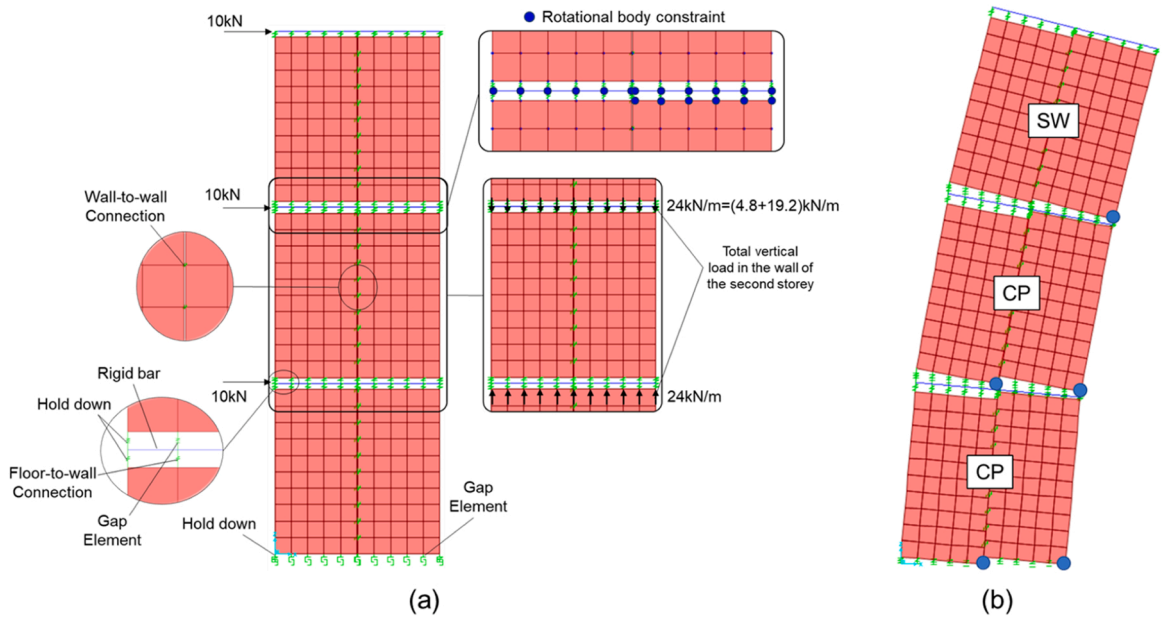

Fig. 12. Three-storey two-panel shear-wall: undeformed configuration (a), deformed configuration (b).

Table 2
The results obtained from the developed equations and numerical models for the three-storey example multi-panel CLT shear-walls.

Storey	Lateral displacement	Analytical models	Numerical models	Discrepancy	Expected kinematic mode	Achieved kinematic mode
1st	$d_{S,1}$ (mm)	3.7	3.7	0.2%	CP	CP
2nd	$d_{S,2}$ (mm)	8.7	9.1	4.6%	CP	CP
3rd	$d_{S,3}$ (mm)	14.4	15.1	5.2%	SW	SW

terms of lateral displacements and load distribution of the analyzed CLT wall system, and it was shown that the analysis demonstrated high accuracy level of the developed analytical equations for lateral deflection calculations of CLT wall systems.

CRediT authorship contribution statement

Daniele Casagrande: Conceptualization, Data curation, Formal analysis, Investigation, Project administration, Supervision, Writing – original draft, Writing – review & editing. **Giuseppe D'Arenzo:** Conceptualization, Data curation, Formal analysis, Investigation, Methodology, Software, Writing – original draft, Writing – review & editing. **Mohammad Masroor:** Data curation, Formal analysis, Investigation, Methodology, Software, Writing – original draft. **Igor Gavrić:** Data curation, Methodology, Writing – original draft. **Ghasan Doudak:** Conceptualization, Project administration, Supervision, Writing – original draft, Writing – review & editing.

Declaration of Competing Interest

The authors declare that they have no known competing financial interests or personal relationships that could have appeared to influence the work reported in this paper.

Acknowledgments

The authors would like to thank Dr. Marjan Popovski from FPInnovations (Canada) for sharing the experimental data used for the validation of the analytical methodology presented in the paper. Parts of this publication are based upon work from COST Action CA20139 "Holistic design of taller timber buildings – HELEN, supported by the European Cooperation in Science and Technology (COST).

Appendix A. Supporting information

Supplementary data associated with this article can be found in the online version at doi:10.1016/j.istruc.2024.106490.

References

[2] Brandner R, Dietsch P, Droscher J, Schulte-Wrede M, Kreuzinger H, Sieder M. Cross laminated timber (CLT) diaphragms under shear: Test configuration, properties and design. Constr Build Mater 2017;157:312–27.
[3] Brandner R, Flatscher G, Ringhofer A, Schickhofer G, Thiel A. Cross laminated timber (CLT): overview and development. Eur J Wood Prod 2016;74:331–51. https://doi.org/10.1007/s00107-015-0999-5.
[4] Casagrande D, Rossi R, Sartori T, Tomasi R. Proposal of an analytical procedure and a simplified numerical model for elastic response of single-storey timber shear-walls. ISSN 0950-0618 Constr Build Mater 2016;Volume 102:1101–12. https://doi.org/10.1016/j.conbuildmat.2014.12.114.
[5] Casagrande D, Doudak G, Mauro L, Polastri A. Analytical approach to establishing the elastic behavior of multipanel CLT shear-walls subjected to lateral loads. J Struct Eng 2018;144(2):04017193.
[6] CSA O86–19 (2019) Engineering design in wood. CSA Group, Mississauga, Canada.
[7] CSI (2017) SAP 2000. Computers and Structures Inc., CA, USA.
[8] D'Arenzo G, Casagrande D, Polastri A, Fossetti M, Fragiacomo M, Seim W. CLT shear walls anchored with shear-tension angle brackets: experimental tests and finite-element modeling. J Struct Eng 2021;Volume 147(Issue 7):04021089. https://doi.org/10.1061/(ASCE)ST.1943-541X.0003008.
[9] D'Arenzo G, Schwendner S, Seim W. The effect of the floor-to-wall interaction on the rocking stiffness of segmented CLT shear-walls. Eng Struct 2021;Volume 249: 113219. https://doi.org/10.1016/j.engstruct.2021.113219.
[10] EN 1995–1-1 (2004) Eurocode 5: Design of timber structures—part 1–1: general rules and rules for buildings. CEN, Brussels, Belgium.
[12] Flatscher G., Schickhofer G. (2016) Displacement-based determination of laterally loaded Cross Laminated Timber (CLT) wall systems. Proceedings of the 3rd INTER Meeting - INTER/49–12-1, Graz.
[13] Gavric I, Fragiacomo M, Ceccotti A. Cyclic behaviour of CLT wall systems: experimental tests and analytical prediction models. J Struct Eng 2015 2015;141. https://doi.org/10.1061/(ASCE)ST.1943-541X.0001246.
[14] Gavric I, Fragiacomo M, Popovski M, Ceccotti A. Behaviour of cross-laminated timber panels under cyclic loads. Materials and joints in timber structures: recent

development of technology, RILEM Book series, vol. 9. Dordrecht: Springer. cop.,; 2014. p. 689–702. DOI: 10.1007/978-94-007-7811-5_62.
[15] Gavric I, Popovski M. Design models for CLT shear-walls and assemblies based on connection properties. Proceedings of the International Network on Timber Engineering Research. UK: Bath; 2014. p. 267–80.
[16] Hummel J, Seim W, Otto S. Steifigkeit und Eigenfrequenzen im mehrgeschossigen Holzbau. Bautechnik 2016;93:781–94. https://doi.org/10.1002/bate.201500105.
[17] Kode A, Amini MO, van de Lindt JW, Line P. Lateral load testing of a full-scale cross-laminated timber diaphragm. Pract Period Struct Des Constr 2021;vol. 26(2): 04021001.
[18] Lam F, Haukaas T, Ashtari S, Haukaas T. in-plane stiffness of cross-laminated timber floors. World Conf Timber Eng 2014:1–10.
[19] Line P, Nyseth S, Waltz N. Full-scale cross-laminated timber diaphragm evaluation. I: design and full-scale diaphragm testing. J Struct Eng 2022;vol. 148(5):1–13.
[20] Lukacs I, Björnfot A, Tomasi R. Strength and stiffness of cross-laminated timber (CLT) shear-walls: state-of-the-art of analytical approaches. Eng Struct 2019; volume 178:136–47. https://doi.org/10.1016/j.engstruct.2018.05.126.
[21] Masroor M, Doudak G, Casagrande D. The effect of bi-axial behaviour of mechanical anchors on the lateral response of multi-panel CLT shear-walls. Eng Struct 2020;Volume 224:111202. https://doi.org/10.1016/j.engstruct.2020.111202.
[22] Masroor M. (2023) Behaviour and design considerations for Multi-panel CLT Shear-walls, PhD thesis University of Ottawa.
[23] Moroder D, Smith T, Pampanin S, Palermo A, Buchanan AH. Design of floor diaphragms in multi-storey timber buildings. Journal 2015;vol. 23(2).
[24] Pei S., Popovski M., Van De Lindt J.W. (2012) Seismic design of a multi-story cross laminated timber building based on component level testing. World Conference on Timber Engineering 2012, WCTE 2012, 2, pp. 244–252.
[25] Pei S, van de Kuilen J-WG, Popovski M, Berman JW, Dolan JD, Ricles J, et al. Cross Laminated Timber for seismic regions: progress and challenges for research and implementation. E2514001 J Struct Eng 2016;142(4). https://doi.org/10.1061/(ASCE)ST.1943-541X.0001192.
[26] Polastri A, Casagrande D. Mechanical behaviour of multi-panel cross laminated timber shear-walls with stiff connectors. Constr Build Mater 2022;Volume 332: 127275. https://doi.org/10.1016/j.conbuildmat.2022.127275.
[27] Popovski M., Schneider J., Schweinsteiger M. (2010) Lateral load resistance of cross-laminated wood panels) 11th World Conference on Timber Engineering 2010, WCTE 2010, 4, pp. 3394–3403.
[30] Reynolds T, Foster R, Ramage M, Bregulla J, Chang W-S, Harris R. Lateral-load resistance of cross-laminated timber shear-walls. J Struct Eng 2017;143(13). https://doi.org/10.1061 /(ASCE)ST.1943-541X.0001912.
[31] Ruggeri EM, D'Arenzo G, Fossetti M, Seim W. Investigating the effect of perpendicular walls on the lateral behaviour of Cross-Laminated Timber shear walls. Structures 2022;46(2022):1679–95. https://doi.org/10.1016/j.istruc.2022.10.141.
[32] Ruggeri EM, D'Arenzo G, Fossetti M. Investigating the effect of the structural interactions due to floors and lintels on the lateral response of multi-storey Cross-Laminated Timber shear walls. Eng Struct 2023;2023(290):116327.
[33] Salvadori V. (2021) Multi-Storey Timber-Based Buildings: An International Survey of Case-Studies with Five or ore Storeys Over the Last Twenty Years. PhD thesis, Vienna University of Technology.
[35] Shahnewaz M, Tannert T, Shahria Alam M, Popovski M. In-plane stiffness of cross-laminated timber panels with openings. Struct Eng Int 2017;27(2):217–23. DOI: 10.2749/101686617X14881932436131.
[36] Tamagnone G, Rinaldin G, Fragiacomo M. A novel method for non-linear design of CLT wall systems. Eng Struct 2018;Volume 167:760–71. https://doi.org/10.1016/j.engstruct.2017.09.010.
[37] Tamagnone G, Rinaldin G, Fragiacomo M. Influence of the floor diaphragm on the rocking behavior of CLT walls. J Struct Eng 2020;146(2020):1–11. https://doi.org/10.1061/(ASCE)ST.1943-541X.0002546.
[39] White Arkitekter (2021) Sara Cultural Centre in Skellefteå, Sweden. A Magnificent State-Of-The-Art Green Building. https://www.theplan.it/eng/architecture/sara-cultural-centre-in-skellefte%C3%A5-sweden-a-magnificent-state-of-the-art-green-building.